ACS APPLIED MATERIALS & INTERFACES

Research Article

www.acsami.org

Anhydrous Proton Conducting Materials Based on Sulfonated Dimethylphenethylchlorosilane Grafted Mesoporous Silica/Ionic Liquid Composite

Ibrahim Saana Amiinu,[†] Xinmiao Liang,[‡] Zhengkai Tu,[†] Haining Zhang,[*,†,§] Jiwen Feng,[‡] Zhongmin Wan,[∥] and Mu Pan[†,§]

[†]State Key Laboratory of Advanced Technology for Materials Synthesis and Processing, Wuhan University of Technology, Wuhan, P. R. China, 430070

[‡]Wuhan Institute of Physics and Mathematics, The Chinese Academy of Sciences, P. R. China, 430071

[§]Hubei Key Laboratory of Fuel Cells, Wuhan University of Technology, Wuhan, P. R. China, 430070

[∥]School of Physics, Hunan Institute of Science and Technology, Yueyang, P. R. China, 414006

ABSTRACT: Efficient membrane proton conductivity at elevated temperatures (>100 °C) and reduced humidification conditions is a critical issue hindering fuel cell commercialization. Herein, proton conducting materials consisting of high surface area acid catalyzed mesoporous silica functionalized with sulfonated dimethylphenethylchlorosilane was investigated under anhydrous conditions. The organic moiety covalently bonded to the silica substrate via active hydroxyl groups on the silica pore surface. The structure and dynamic phases of the attached organic molecule were characterized and qualitatively determined by XRD, TEM, FT-IR, and solid state NMR. The amount of grafted organic molecules was estimated to be 2.45 μmol m^{-2} by carbon elemental analysis. The so-formed composite materials showed adequate thermal stability up to 300 °C as determined by TGA. Under anhydrous conditions, ionic conductivity of the composite material upon ionic liquid impregnation reaches a peak value of 1.14×10^{-2} S cm^{-1} at 160 °C associated with the activation energy of 9.24 kJ mol^{-1} for proton transport.

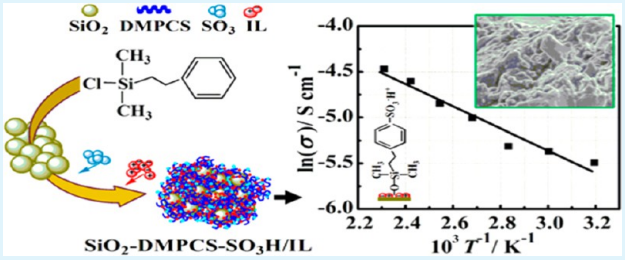

KEYWORDS: *proton conducting materials, mesoporous silica, ionic liquid, charge transfer, elevated temperature*

INTRODUCTION

Energy forms the basis of 21st century industrialized society, powering our homes, workplaces, devices, transportation, and communication systems. However, as concerns mount on limited energy resources, rapid climate change, and air and environmental pollution on account of burning fossil fuels, new sustainable sources of energy turn out to be a viable alternative for a safe future energy generation.[1] The need for renewable and environmentally friendly sources of energy to meet changing and growing global energy demands is the motivation behind the green energy revolution.[2,3] Fuel cells, particularly the proton exchange membrane fuel cell (PEMFC), emerge as a potential practical alternative to depleting fossil energy resources due to its green nature and high power density.[4,5]

Currently, PEMFCs are generally operated at temperatures below 80 °C with humidified gases as restricted by a proton conduction mechanism. The thus-applied large radiator and humidification subsystem can lead to decreased power density as well as increased cost of the PEMFC system, which still remain as major impediments to PEMFC commercialization. Operation of a PEMFC at elevated temperature (above 100 °C) under reduced humidification conditions has been realized as an effective approach to simplifying water and heat management, increasing electrode catalytic activity and reaction kinetics, and enhanced tolerance of carbon monoxide in fuel gases.[6,7] The water-thermal management constraints of a cooling system as required in low temperature PEMFCs is also assuaged.[8]

One of the technical challenges for a PEMFC operated at elevated temperatures is the membrane electrolyte that should maintain reasonable transport at such operation conditions. The commercially available perfluorosulfonated membranes (Nafion from DuPont or Aquivion from Solvay Solexis) exhibit poor ionic conductivity at elevated temperatures (above 100 °C) under low humidity coupled with high vulnerability to chemical degradation at these extreme conditions, as well as large volumetric change or shrinkage with humidity, which still remain as a drawback to PEM fuel cell commercialization.[9,10] Conversely, researchers believe that to optimize the performance of PEM fuel cells it is necessary to design an electrolyte membrane with robust proton conducting properties at elevated temperatures and low humidity without compromising structural stability. Notably, organic–inorganic composites have been on the hit list of potential materials in the design trail.

Received: May 14, 2013
Accepted: October 30, 2013
Published: October 30, 2013

More recently, silica-organic-based composite materials have drawn much research interest as intriguing materials for fuel cell application.[11] Nafion, polyvinylidene fluoride, and poly(ether sulfone) impregnated with inorganic oxides (TiO_2, SiO_2, ZrO_2, etc.) are among the materials in recent work on composite electrolyte membranes for elevated temperature fuel cell applications.[12−18] Effective proton transport is known to be highly dependent on the degree of hydration, which favors proton conductivity in perfluorinated sulfonic acid electrolyte membranes such as Nafion.[19,20] The advantages for PEMFC operated at elevated temperature seem reachable in a silica-organic composite membrane which combines the hygroscopic/hydrophilic properties of the silica, the easiness of aromatic sulfonation and reactivity of the copolymer, and thermochemical stability.

Acid catalyzed sol−gel synthesized mesoporous silica exhibits high hydrophilicity due to the large numbers of surface hydroxyl (≡Si−OH) groups.[21] Surface hydroxyl groups play a pivotal role as intermediates for stable chemical bond formation and function as anchoring points for attachment or adsorption of organic molecules through silane bridges between the silica substrate and the organic moieties.[22−24] Mesoporous silica is reported to facilitate back diffusion of water, increase water concentration at the anode catalyst layer, and reduce anode over potential which facilitates water uptake and/or retention under low humidity/high temperature operation conditions, thus enabling a more stable and reversible current−voltage response.[25−27] Furthermore, surface modification of mesoporous silica with ionic groups including sulfonic acid,[28−30] phosphonic acid,[31,32] and heterocyclic groups[33,34] has been reported for the enhancement of ionic conductivity. However, the ionic conductivity of surface modified mesoporous silica is also strongly dependent on relative humidity. For example, Wark and co-workers reported that the proton conductivity of sulfonic acid functionalized mesoporous silica increased from about 10^{-4} S cm^{-1} to about 0.2 S cm^{-1}, while the relative humidity varied from 0 to 100% at 140 °C.[29] Ionic liquids are often considered as good anhydrous proton conductors. Doping composite membranes with ionic liquid often results in improved thermostability and electrochemical properties which are required for long-term cell performance.[35] However, it was found that protic-ionic-liquid-modified mesoporous silica still requires certain humidification conditions to achieve reasonable proton conductivity (0.05 S cm^{-1} under relative humidity of 30% at 90 °C).[34] It should be pointed out that increased uptake of water in the membrane would require efficient water management techniques so as to avoid electrode flooding and membrane over swelling induced volumetric change, which often lead to hydrophobic/hydrophilic nanophase separation by liquid water accumulation, in which reaction kinetics are impeded, resulting in poor cell performance.[36] Thus, development of anhydrous proton conducting materials is of importance for increasing durability and decreasing complexity of PEMFC systems.

In this manuscript, we describe the preparation of an efficient proton conductive composite membrane based on sulfonated high surface area acid catalyzed mesoporous silica functionalized with a silane molecule (dimethylphenethylchlorosilane) via a simple post-synthesis sol−gel route. The membrane is evaluated for thermal decomposition of chemical components and tested for ionic conductivity, based on the influence of sulfonic acid groups and ionic liquid, over a wide range of temperatures (40−160 °C) under nonhumidity dependent conditions. In addition, the membrane is characterized to determine the chemical structure, morphological properties, and elemental composition of the different phases.

EXPERIMENTAL SECTION

Materials and Method. All chemical reagents were of analytical grade. Styrene (98%, Shanghai Reagent Co., China) was washed with 10% aqueous sodium hydroxide to remove the phenolic inhibitor (4-*tert*-butylcatechol), dried over sodium sulfate anhydrous, and distilled under reduced pressure. Toluene (99.5%, Sinopharm Chemical Reagent Co. Ltd., China) was dried by refluxing over sodium metal using benzophenone (Sinopharm Chemical Reagent Co. Ltd., China) as an indicator prior to distillation. Dry toluene was stored over a molecular sieve until used. Ionic liquid (IL), 1-butyl-3-methylimidazolium tetrafluoroborate (BuMeImBF4, 99%), was purchased from Chengjie Chem. Ltd. (Shanghai, China) and used without purification. All other solvents and chemical reagents including tetraethoxysilane (TEOS-98%, Sinopharm Chemical Reagent Co. Ltd., China), dimethylchlorosilane (DMCS, 97%, Alfa Aesar, Lancaster), and triethylamine (99%, Shanghai Reagent Co., China) were of reagent grade and used as received.

Synthesis of Well Ordered Mesoporous Silica Particles. Nonionic triblock copolymer $EO_{106}PO_{70}EO_{106}$ (pluronic F-127, BASF, Sigma) was employed as a structure directing agent (SDA) and tetraethoxysilane (TEOS) as the silica precursor. Periodic mesoporous silica particles were prepared via a sol−gel process as described elsewhere.[37] Briefly, 1.70 g of F-127 was dissolved by stirring in 80 g of deionized water and 3.5 g of concentrated hydrochloric acid (36 wt % HCl). A total of 4.0 g of buthanol was added to the reaction mixture and stirred continuously until a homogeneous solution was formed. The solution was subsequently heated to 45 °C, and TEOS was quickly added under vigorous stirring. The stirring rate was reduced and the reaction sustained for 24 h. The mixture was then transferred into a hydrothermal reactor for another 24 h at 100 °C without agitation. Well ordered mesoporous silica with a uniform pore size was obtained subsequent to filtration, refluxing in ethanol/HCl solution for 24 h to remove structure directing agent, and drying at 60 °C.

Preparation of Dimethylphenethylchlorosilane. Dimethylphenethylchlorosilane (DMPCS) was synthesized in a catalytic hydrosilylation reaction of dimethylchlorosilane (DMCS) to styrene in the presence of H_2PtC_6. Preparation of DMPCS was carried out akin to literature[38] but for the stirring and heat treatment schemes. Typically, styrene, dimethylchlorosilane, and dry toluene were reacted in a mass ratio of 2.0:1.8:1.0, respectively. A total of 0.005 mL of acetic acid was added to the reaction mixture and heated overnight at 55 °C in an oil bath under mild stirring. The molecular framework of the product has one silicon atom bonded to the aromatic ring via two ethylene groups with one chlorine atom directly bonded to the silicon atom as shown in Scheme 1.

DMPCS Functionalized Silica. Dimethylphenethylchlorosilane was grafted onto the silica pore walls in a salinization reaction via the covalently attached silanol groups on the silica pore surface as anchor points. As-synthesized silica particles were reacted with the prepared DMPCS and dry toluene. In the reaction process, 1.0 g of silica nanoparticles was dried at 110 °C and dispersed in 20 mL of solution of each DMPCS and toluene. The mixture was sonicated for 30 min and then stirred constantly at 85−110 °C for 24 h in a triethylamine medium under a nitrogen atmosphere. The reaction yielded a DMPCS grafted silica nanoparticle (SiO_2−DMPCS). Ungrafted organic residue was sluiced out by dispersion in toluene and then centrifuged several times. Solid particles were recovered by precipitation in methanol and dried at 60 °C in a vacuum. Ionic liquid (IL) (BuMeImBF4, 99%) was added (IL/SiO_2−DMPCS = 1/1.4 weight ratio) to the SiO_2−DMPCS by solvent blending and agitated for 30 min before solvent evaporation at 80 °C for 36 h. Prior to the addition of IL, the SiO_2−DMPCS nanoparticles were solfonated via electrophilic aromatic substitution with concentrated sulfuric acid to obtain a terminated sulfonic ($SO_3^-H^+$) end group entrapped in the phenyl group.

Scheme 1. Synthesis Schematics of Sulfonated SiO_2–DMPCS Composite Membrane Embedded with Ionic Liquids

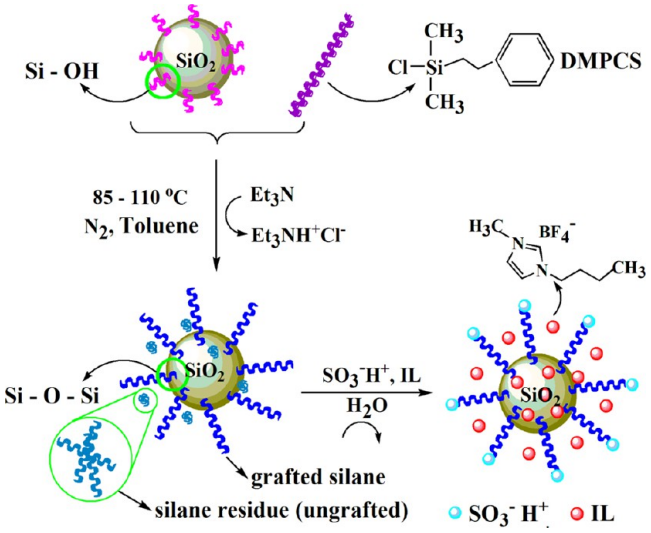

In the sulfonation process, SiO_2–DMPCS particles were dispersed in concentrated sulfuric acid (H_2SO_4, 98%) and vigorously stirred at room temperature over a period of 12 h. Finally, the solid particles were retrieved and washed repeatedly with deionized water until a neutral pH was observed. The sulfonated composite nanoelectrolyte membrane consisting of imidazolium type IL and SiO_2–DMPCS was finally heated to 100 °C for 1 h before measurement of electrochemical properties. The synthesis schematic is depicted in Scheme 1.

Characterization. In this experiment, three samples consisting of bare mesoporous silica, DMPCS modified silica, and IL–DMPCS modified silica were characterized for microstructure and morphology, and three samples consisting of sulfonated–DMPCS modified silica, unsulfonated–DMPCS modified silica, and sulfonated–IL–DMPCS modified silica were tested for electrochemical properties.

Typically, small-angle X-ray diffraction (SAXRD) patterns of mesoporous silica particles and modified silica were recorded on a Rigaku D/MAX-RB diffractometer with Cu Kα radiation operating at 40 kV and 50 mA. In the transmission electron microscopy (TEM) measurement, fine particles of the samples were first dispersed in ethanol and sonicated in a water bath for 10 min at room temperature. A drop of the suspension was then placed on a thin carbon film supported by a copper grid. TEM images were finally obtained using high resolution electron microscopy (JEM-2010FEF). Solid state proton nuclear magnetic resonance (^{1}H NMR) spectra were acquired by magic angle spinning on a Mercury VX-300 (Varian, USA). Proton conductivity measurements of the compacted pellets formed under a pressure of 15 MPa of composite electrolytes were carried out using a potentiostatic impedance frequency response analyzer (Autolab PG30/FRA, Eco Chemie, The Netherlands), operating at a 10 mV signal amplitude over a frequency range of 10 Hz–100 kHz with a model cell of 5 cm electrode diameter. The prepared compacted pellet was sandwiched between the Pt electrodes and heated from 25 to 170 °C without applied pressure. Electrochemical stability of the electrolyte relative to proton conductivity was carried out under an elevated heat cycle between 80 and 160 °C. In a second cycle, the membrane was soaked in deionized water under stirring at room temperature before electrochemical measurements. Infrared spectra were obtained using a Fourier transform infrared spectrometer (FT-IR, Bio-Rad FTS 300) with a resolution of 2 cm^{-1} from 450 cm^{-1} to 4000 cm^{-1} as a means of investigating the interaction between the silica host, IL, and the silane molecule. In situ FT-IR spectra of the membranes were also acquired with a KBr pellet technique successive to high temperature proton conductivity measurements. Scanning electron microscopy (SEM; Hitachi S-4800 Tokyo, Japan) was performed to ascertain the surface characteristics and morphology of the composite materials. BET characteristics were measured using an accelerated surface area and porosity analyzer (ASAP 2020, Micromeritics). Both Carbon Elemental Analysis (CEA) and Thermogravimetric Analysis (TGA) were performed using an Elemental Analysis system (GmbH VarioEL) and NETZSCH STA 449 F3 Jupiter thermal analyzer, respectively. The TGA heating rate was 10 °C per min over a temperature range of 25–800 °C under a nitrogen atmosphere.

RESULTS AND DISCUSSION

Mesoporous silica substrates were prepared through the sol–gel process assisted with a structure directing agent, the nonionic triblock copolymer $EO_{106}PO_{70}EO_{106}$, according to the literature.[37] The small-angle X-ray diffraction pattern of the unmodified mesoporous silica particles, Figure 1a, shows one

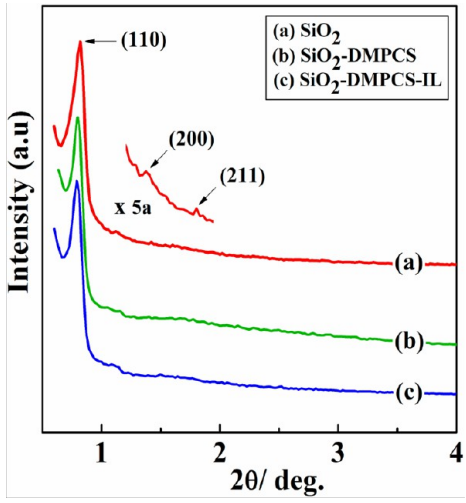

Figure 1. Small angle X-ray diffraction pattern of (a) SiO_2, (b) SiO_2–DMPCS, and (c) SiO_2-DMPCS/IL.

intense peak corresponding to diffraction at (110) and two fairly weak peaks at (200) and (211) within low angles of 2θ (0.5–2°). The d(110) spacing is ~11.4, which is equivalent to a 16.1 nm unit cell parameter. The intense peak correlates to long-range ordered mesopores of the silica material as a result of characteristic 3D connectivity of cubic morphology. This suggests the type of silica material as SBA-16.[39] The TEM images in Figure 2 reveal a wide range of well ordered cubic structures in harmony with the XRD results. The ordering of cubic morphology of the silica remained fairly intact in the modified materials which showed similar diffraction patterns indicating structural stability of the silica mesostructure. However, a slight decrease in diffraction intensity observed for the modified materials corresponds to pore surface functionalization by the organic moieties. Indeed, this class of silica material has become a focus of research due to the long-range ordering of 3-D caged-like mesostructure (cubic, $Im3m$), high specific surface area, and large number of surface silanol groups, which make them potential materials for application in molecular adsorption, catalysis, and sensors.[40,41] The structural configuration and local chemical environment of the mesoporous silica prior to grafting was probed by solid state ^{29}Si and ^{13}C CP MAS NMR to qualitatively determine the surface species, state of TEOS hydrolysis, and the cross-linking of a silica network. The three prominent peaks observed in Figure 3a are attributed to the silicon atomic site for germinal silanols (Q^2), isolated silanols (Q^3), and siloxane bridges (Q^4) at −92.4, −101.6, and −109.7 ppm chemical shifts, respectively. In Figure

dx.doi.org/10.1021/am404417g | ACS Appl. Mater. Interfaces 2013, 5, 11535–11543

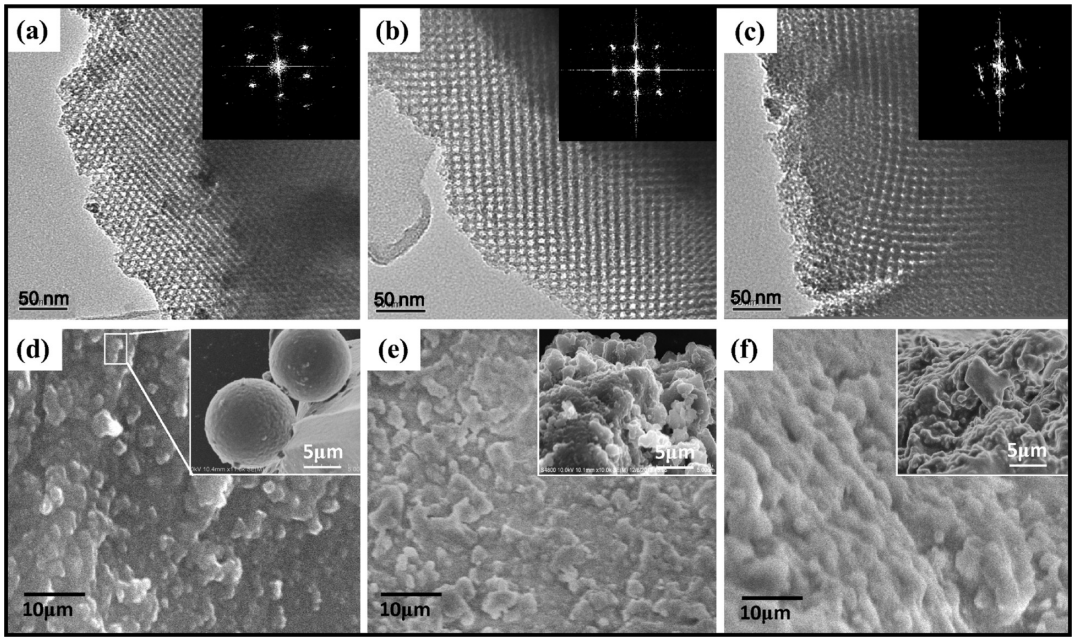

Figure 2. HR-TEM (inset is Fourier diffractogram) and SEM morphology of (a, d) mesoporous SiO_2, (b, e) SiO_2–DMPCS, and (c, f) SiO_2–DMPCS/IL embedded with ionic liquid, respectively.

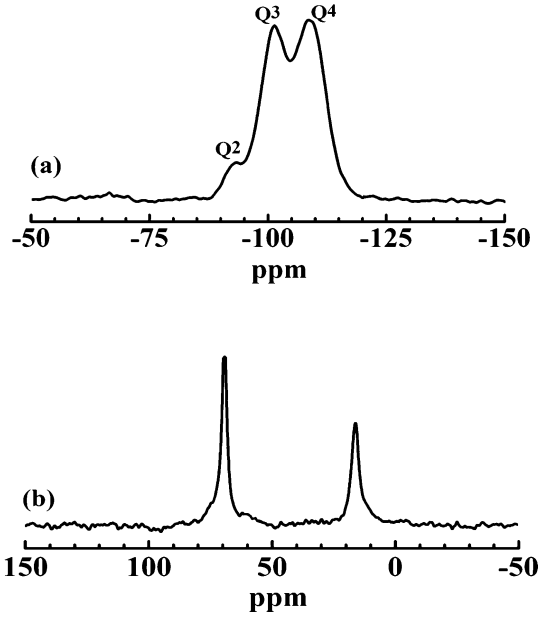

Figure 3. (a) ^{29}Si MAS NMR and (b) ^{13}C CP MAS NMR spectra of bare mesoporous silica.

3b, the spectrum shows resonance peaks at 16.2 and 70.7 ppm ascribable to carbon atoms of methyl and ethylene groups of surfactant molecules that adhered to the silica pores during solvent extraction or from incomplete hydrolysis of the TEOS precursor. This may account for the presence of carbon in the mesoporous silica. However, the repeated washing of the samples at various phases with water and organic solvents could assist in final removal of the remaining entrapped surfactant. That notwithstanding, the results showed that the as-synthesized mesoporous silica possesses the desired chemical framework adequate for further organo-chemical surface modifications and processing.

A DMPCS molecule is attached to the silica pore surface via silane chemistry either by two neighboring Si–OH groups on the silica surface or by one surface silanol and a neighboring alkoxysilane molecule.[42] Grafting of functional DMPCS onto the silica surface was qualitatively determined by both FT-IR and solid state ^{1}H MAS NMR, which revealed detailed information about the molecular structure and dynamic behavior of the bonded phases. The IR spectra of the unmodified and grafted silicas are reported in Figure 4. The spectrum of grafted silica shows characteristic stretch vibrations

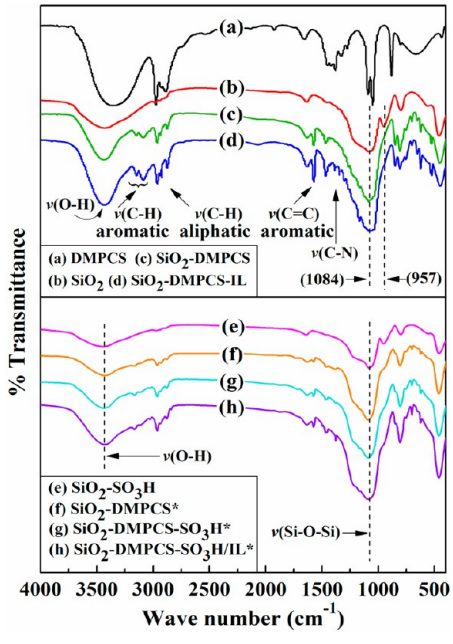

Figure 4. FT-IR spectra of (a) DMPCS, (b) SiO_2, (c) SiO_2–DMPCS, (d) SiO_2–DMPCS/IL, (e) SiO_2–SO_3H, (f) SiO_2–DMPCS*, (g) SiO_2–DMPCS–SO_3H*, and (h) SiO_2–DMPCS–SO_3H/IL*. An asterisk indicates in situ high temperature measurements.

of aliphatic groups ν(C−H) at 2875, 2936, and 2962 cm^{-1} as well as weak-to-moderate bands of aromatic groups of ν(C−H) at 3087 and 3149 cm^{-1} and ν(C═C) at 1573 cm^{-1} of the DMPCS framework. Compared with the unmodified silica, these additional peaks are absent, which suggests silane coverage of the silica surface. Grafting is further endorsed by the major decrease in band intensity or disappearance of the hydroxyl groups (Si−OH) at 957 cm^{-1} observed for the SiO_2−DMPCS composite. The decrease in band intensity of δ(O−H) at 1637 cm^{-1} is indicative of reduced surface hydration, which is in conformity with TG analysis. However, the strong absorbance at 1084 cm^{-1} is ascribed to a ν(Si−O−Si) stretch vibration of the silica network. The CN stretching vibration of the imidazolium core, ν(C═N), typically in the range 1400−1650 cm^{-1}, and ν(N−H) in the spectrum of SiO_2−DMPCS-IL are not clearly seen due to overlap with absorption peaks of ν(C═C) and ν(O−H), respectively. However, the weak peaks at 1060−1380 cm^{-1} are ascribed to the ν(C−N) stretching vibration. In order to authenticate anhydrous proton conductivity, in situ high temperature FT-IR was also carried out to verify the existence of H_2O molecules on the surface of the mesopores. The in situ spectra of all electrochemical samples are shown in the same figure. It is imperative to note that the close proximity of the hydrophobic phenyl group of the DMPCS framework to the sulfonic group may play the role of shielding the acid site against water and possibly reduce the effects of physisorbed water on acidity and proton migration activity. The shielding effect makes a majority of existing physisorbed water molecules within the mesopores of the membrane neutral molecules. Therefore, an ex situ characterization, shown in the figure, was carried out on bare and sulfonic acid treated silica to evaluate the interaction of surficial Si−OH groups with $-SO_3H$ and water molecules in vitro in the SiO_2−DMPCS composite domain. Sulfonic acid groups are considered to interact preferentially with Si−OH groups and physisorbed water on the surface of mesoporous silica. Even so, the existence of a sulfonic acid group is not apparent. Be that as it may, the spectra show that the −OH characteristic band at ∼3446 cm^{-1} broadened after sulfonation as a result of the stretching vibration of the $-SO_3^-$ group. The widening of peaks seems to suggest the existence of strong hydrogen bonds owing to the interaction between surficial −OH groups and sulfonic molecules. However, the absorption band of the S═O stretching vibration within 1000−1350 cm^{-1} coincides with the strong band of symmetric and asymmetric vibration of the Si−O−Si network and remained obstructed. Consequently, IR could not provide the platform to clearly evaluate the interaction of sulfonic acid groups with surficial Si−OH or physisorbed water in the composite materials.

Solid state ^{1}H MAS NMR was employed to verify the different active H atoms prompted by the sulfonic acid group, chemisorbed/physisorbed water, and the aromatic fragments of the composite material. By visual inspection, one could draw a qualitative conclusion to uphold the prevalence of organic molecular grafting. The spectrum of bare silica, Figure 5a, shows a chemical shift at 3.5 ppm associated with surface silanols that H-bonded to physisorbed molecular water typical of periodic mesoporous silicas. The weak peak at ∼1.67 ppm is assigned to H atoms of isolated silanols. In the modified silica, Figure 5b, a chemical shift of aromatic H atoms of the phenyl framework occurs at $\delta \approx 7.3$ ppm, which indicates the covalent attachment of the DMPCS molecule to the silica surface. The spectrum at $\delta \approx 0$ ppm results from the H atoms of the

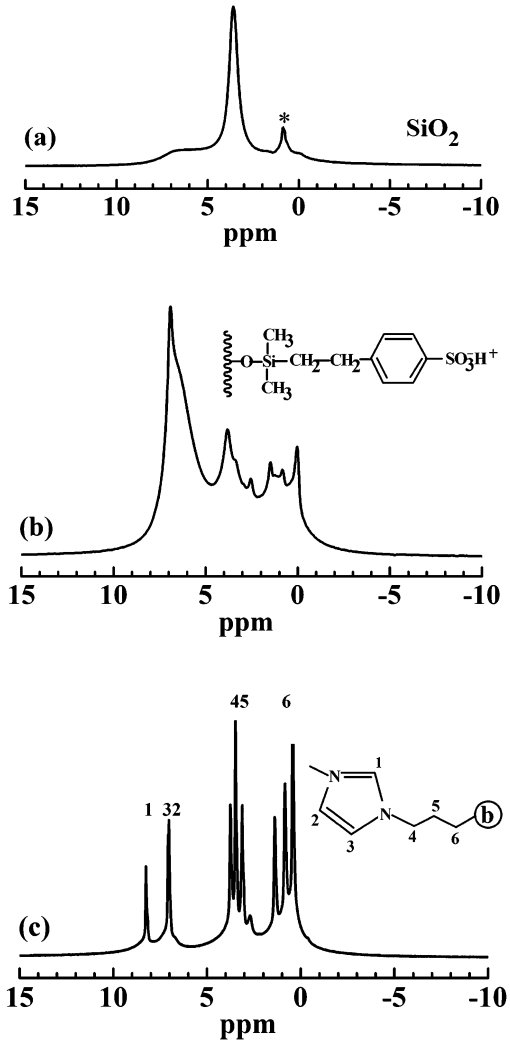

Figure 5. Solid state ^{1}H MAS NMR spectra of (a) SiO_2, (b) SiO_2−DMPCS, and (c) SiO_2−DMPCS/IL composite.

terminal methyl groups directly bonded to the silicon atom (−Si−CH_3). The signals at $\delta \approx 0.8$ ppm and $\delta \approx 1.6$ ppm are attributed to H atoms of the methylene group attached to the silicon atom (−Si−CH_2−) and the H atoms of the methylene group adjacent to the aromatic ring (−CH_2−Ph−), respectively. The occurrence of these H atomic pointers further confirms the FT-IR results of a successful grafting. The chemical shift at about 3.2 and 3.9 ppm is due to H atoms from the $-SO_3H$ group and residual water, respectively.[43] The peak at $\delta \approx 2.6$ ppm is identified to originate from H atoms of surface Si−O*H* groups due to an incomplete salinization reaction.[22,44] However, the relatively low intensity of the peak indicates that only a small number of surface silanol groups remained on the mesoporous silica after silane functionalization. The addition of IL introduces well resolved peaks at 8.41 and 7.16 ppm, Figure 5c, for H atoms of (−NC*H*N−) and (−NCHC*H*N−), respectively. All the same, the H atoms peak for the phenyl framework of SiO_2-DMPCS remained but coincides with the H atom chemical shift of (−NC*H*CHN), analogous to FT-IR observation.

The N_2 adsorption−desorption (A−D) isotherm and pore size distribution of bare and silane modified silica were measured at −196 °C and are reported in Figure 6. The A−D isotherms, Figure 6B, showed type IV hysteresis with total

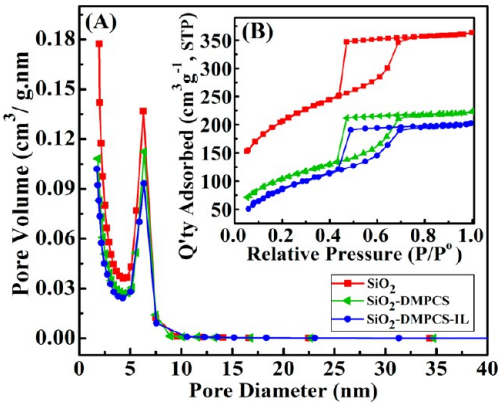

Figure 6. (A) Pore size distribution and (B) nitrogen adsorption–desorption isotherm of mesoporous SiO_2 (–■–), SiO_2–DMPCS (–▲–), and SiO_2–DMPCS/IL (–●–).

pore volume obtained at $P/P_o \approx 0.99$. The hysteresis is indicative of capillary condensation, and closure at $P/P_o \sim 0.42$ signifies the presence of mesopores.[39] The BET specific surface area and pore volume of the silica material reduced significantly upon modification, which reflects the existence of an added organic molecule to the virgin silica. This observation is further investigated and vividly reaffirmed by characteristic weight loss analysis. The structural properties of the materials are given in Table 1.

Table 1. Structural Properties of SiO_2, SiO_2–DMPCS, and SiO_2–DMPCS–IL

	EA	TGA	BET			GD
sample	% C content	weight loss (%)	S_{BET} (m^2g^{-1})	V_p (cm^3g^{-1})	D_p (nm)	δ ($\mu molm^{-2}$)
SiO_2	7.22	13.40	748	0.56	3.01	
SiO_2–DMPCS	24.23	47.84	390	0.34	3.54	2.45
SiO_2–DMPCS-IL		32.76	302	0.31	3.30	

Thermal characteristics of as-synthesized silica, pure DMPCS, SiO_2–DMPCS, and SiO_2–DMPCS/IL are reported in Figure 7. The bare silica and pure DMPCS showed a total weight loss of ~13.4% and ~87.3%, respectively, over the temperature range of 25–600 °C, above which there is no

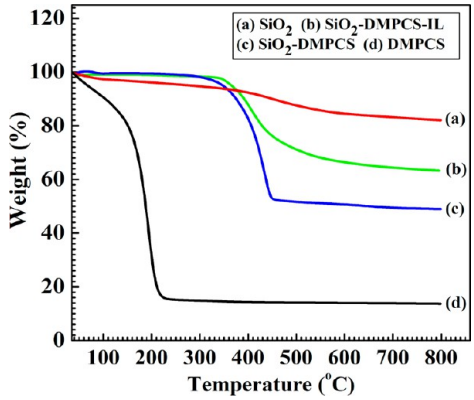

Figure 7. Thermo-gravimetric analysis curves of (a) SiO_2, (b) SiO_2–DMPCS/IL, (c) SiO_2–DMPCS, (d) DMPCS.

further significant loss. However, the silane loaded silica composite shows an initial weight loss of 0.41% within ~150 °C. This weight loss is attributed to thermal desorption of physisorbed water and traces of residual organic solvents, respectively, from the hydrophilic character of the membrane and the solvents used in the syntheses. Beyond this temperature, the material experiences an abrupt weight loss between ~320 and ~450 °C due to thermal decomposition of methyl groups on the Si–O backbone, in this case the DMPCS segment of the SiO_2–DMPCS composite. The material further degrades gradually over the temperature range above ~500 °C at 2.81% as a degradation response of the silane component and/or char-like formation of organic residue. Comparatively, there is minimal initial weight loss in the modified silicas than bare silica, and the converse is true in the region of ~320–600 °C. The former is as a result of decreased surface hydration due to reduced pore volume and/or surface hydrophobicity upon pore wall modification by organic molecules (apolar character), whereas the latter is due to thermal disintegration of the chemically bonded organic molecules. This is in conformity with the general observation that organically modified silica surfaces lead to reduced water uptake characteristics. The ionic liquid doped composite in Figure 7b experiences a relative decrease in initial weight loss but shows a comparatively improved thermal resistance with minimal weight loss. On one hand, the weight loss may be due to the aforementioned reasons. On the other hand, the relatively improved thermal resistance may be attributed to thermal shielding of the pore entrapped silane moieties by the high thermo-resistive silica substrate coupled with the thermal resistant character of the ionic liquid. Since the degradation of the organic molecule occurs above 300 °C, it is obvious that chemical bonding prevailed in the composite material. Consequently, the synthesized composite membranes demonstrated adequate thermochemical stability suitable for high temperature fuel cell application.

To further ascertain attachment of the organic moiety onto the silica pore surface, the amount of attached silane molecules was quantitatively determined via carbon elemental analysis, as also shown in Table 1. The existence of carbon in bare mesoporous silica indicates the incomplete hydrolysis of a TEOS precursor or incomplete removal of structure directing block copolymers from the silica. On the basis of the difference of elemental analysis data for carbon in bare and silane modified silica, the grafting density was calculated to be 2.45 μmol m^{-2} using a previously reported equation,[45] and the grafting distance between two anchored molecules is about 0.82 nm. Steric hindrance, which is often encountered, may not pertain given that the organic molecule is of low molecular weight.

The efficiency and power density of an assembled fuel cell is dependent on the ionic conductivity capacity of the proton conducting electrolytes. To evaluate the proton transport properties of the synthesized composite electrolyte materials, unsulfonated–DMPCS modified silica, sulfonated DMPCS modified silica, and sulfonated DMPCS modified silica impregnated with ionic liquid (BuMeImBF4) were compacted into pellets under a pressure of about 15 MPa. The morphology of compacted pellets examined by SEM is displayed in Figure 2. It can be seen that with the assistance of ionic liquid, no isolated mesoporous silica nanoparticles were observed compared to the bare silica sample, indicating the improved

interfacial contact and the according improved charge transfer resistance by ionic liquids.

Figure 8 illustrates the typical electrochemical impedance response characteristics as a function of temperature for a

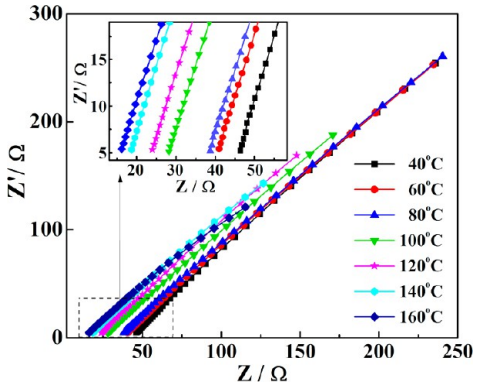

Figure 8. Electrochemical impedance spectra of composite electrolyte embedded with ionic liquids at different temperatures under anhydrous conditions within a frequency range of 10 Hz−100 kHz.

composite electrolyte pellet impregnated with ionic liquid (BuMeImBF4) under anhydrous conditions. Although the full analysis of proton conductivity relies on a model simulation, a visual inspection of the impedance spectra allows us to draw a qualitative conclusion since the intercept at the *X* axis at high frequency reflects the charge transfer resistance. From the temperature-dependent impedance spectra of a composite electrolyte of sulfonated DMPCS modified silica impregnated with ionic liquid, it can be qualitatively concluded that the charge transfer resistance decreases and the proton conductivity increases with the increase in temperature.

The highest ionic conductivity values, by simulation and calculation from impedance spectra, for an unsulfonated membrane (SiO_2−DMPCS), a membrane without IL (SiO_2−DMPCS-SO_3H), and a composite membrane impregnated with IL (SiO_2−DMPCS-SO_3H/IL) were found to be 2.41×10^{-4}, 4.74×10^{-3}, and 1.14×10^{-2} S cm^{-1}, respectively. Although the proton conductivity of the IL impregnated membrane was attained under anhydrous and high temperature conditions, it is comparable to the conductivity observed for Nafion-1100[46] and sulfonic acid functionalized mesoporous silica[29,47] at 140 °C and 20−100% RH conditions. Notably, the proton conductivity of 10^{-2} S cm^{-1} is comparable to that of the well studied anhydrous polybenzimidazole membranes doped with phosphoric acid and is the usual value for practical fuel cell performances.[48] Linear regression of the inverse of temperature versus the logarithm of conductivity is plotted in Figure 9 and used in conjunction with Arrhenius equation to evaluate the activation energies (E_a) associated with the respective membranes. The activation energy is determined to be 9.24, 10.60, and 16.2 kJ mol^{-1} for a composite membrane containing IL, a membrane without IL, and an unsulfonated membrane, respectively. The results suggest that the membrane impregnated with IL which had the lowest charge transfer resistance to proton conductivity also conferred the lowest activation energy. Ionic liquid facilitates the mobility of ionic species (ion exchange) in the membrane as temperature increases, thereby enhancing proton transport properties.[49] Apparently, proton mobility was partly catalyzed by the sulfonic acid groups, which affected an increase in proton conductivity from 2.41×10^{-4} to

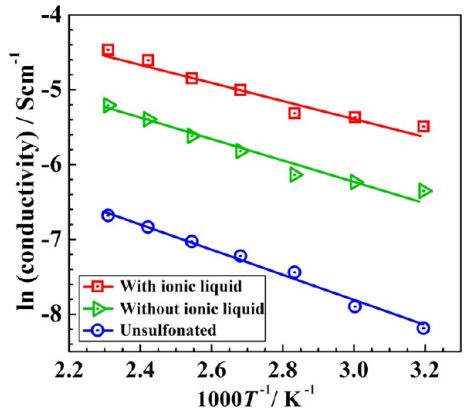

Figure 9. Temperature dependent anhydrous proton conductivity of SiO_2−DMPCS composite electrolytes as indicated in the figure. Solid lines are fits with Arrenhius' equation.

4.74×10^{-3} S cm^{-1}, correspondingly before and after sulfonation. Sulfonic acid groups are entrapped to the acid-functionalized groups (DMPCS segment) anchored to the ordered silica channels. Hydrogen bonding interaction of surficial −OH with sulfonic groups within the membrane, depicted in Scheme 2, results in the formation of a continuous

Scheme 2. H-Bonding Network of Silanols and Sulfonic Acid Groups

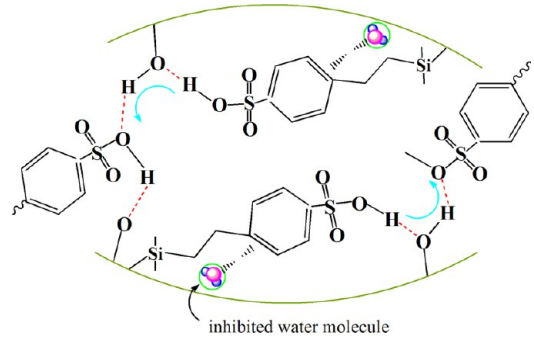

network path, which enables protons to hop from one acid site to its nearest neighbor.[50] TG analysis of the composite material shows that eviction of physisorbed water occurs at about 150 °C, in agreement with previous reports,[21] which is below the temperature at which maximum proton migration was observed. Thus, the highest conductivity at 160 °C may be attributed to the strong ion exchange interaction of ionic liquid and sulfonic acid (SO_3−) groups rather than influenced by physisorbed water molecules. Strong interaction exists between sulfonic acid groups and free silanols compared to those of water molecules given that the hydrophobic character of grafted aromatic moieties inhibits water molecules relative to bare mesoporous silica. It therefore presupposes that the weak proton conductivity observed for SiO_2−DMPCS is due to proton transfer through a hydrogen bonding network of surficial −OH groups.

Aside from the ionic conductivity properties, the membrane containing the IL was also easily fabricated at a rate of 15 MPa/10 min compared to the membranes without IL. This could be attributed to the dispersion of IL, which, besides its ion exchange properties and thermal stability, also reinforces plasticizing effects through Coulombic interaction to aid the

cluster of the fine solid particles,[51] as also confirmed in the SEM investigation. Mesoporous channels of the silica material enhanced the "holding strength" and facilitate the retention of IL through the capillary forces generated within the mesostructure.[52] The holding capacity prevents leaching out of IL, thereby retaining long-term ionic conductivity and cell performance. This could also account for the presence of IL in the composite material even after washing several times. However, the amount of IL retained in the membrane after washing was not determined and could be considered in further research.

Long-term cell performance and durability of a fuel cell system is critically affected by the stability of the electrolyte membrane and electrode catalytic activity. Therefore, the composite membrane was evaluated under an anhydrous state for electrochemical stability by variation of proton conductivity as a function of testing time under the conditions stated in Figure 10. It can be seen that no significant decline in proton

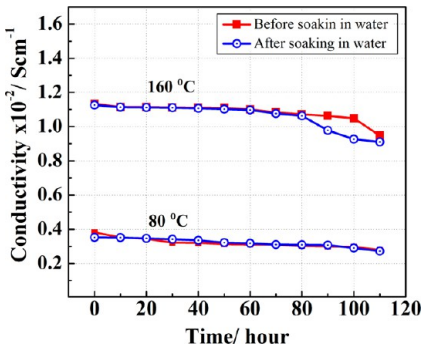

Figure 10. Proton conductivity of a composite electrolyte embedded with ionic liquids as a function of testing time under alternative conditions as indicated in the figure.

conductivity was observed within 80 h/160 °C and 110 h/80 °C, respectively. The steady proton conductivity is associated with the unwavering ion exchange process within the membrane as a result of the strong electrostatic interactive retention of ionic liquid molecules within the mesopores. Hydroxyl groups on the silica surface may interact with IL to form an ordered salvation layer and influence interfacial interactions, layering of ions, and irreversible absorption of ions on the silica surface in the SiO_2−DMPCS/IL nanodispersion. Nevertheless, a slight drop in proton conductivity was observed after 80 h/160 °C and may be attributed to changes in structural properties of the organic moieties by the heat cycles which interrupted the connectivity of proton conducting network path. All the same, the results signify that the prepared composite membrane is reasonably stable and may be useful as electrolyte material for long-term fuel cell applications.

CONCLUSION

We have prepared an organic−inorganic proton conducting membrane material based on ordered mesoporous silica (SBA-16) as a host and dimethylphenethylchlorosilane as an anchoring guest. Mesoporous silica substrates were prepared by the sol−gel process assisted with a nonionic triblock copolymer as a structure directing agent and organically modified via silane chemistry. The results showed that the organic moiety was successfully grafted onto the silica pore surface with a grafting distance between two anchoring sites of 0.8 nm and remained thermally stable up to 300 °C. The periodicity of the silica substrate was also retained after silane functionalization. Both FT-IR and solid state MAS NMR revealed the existence of new phases to confirm the structural bonding of organic fragments in the composite. Ionic liquid retained within the pores of the composite material conveyed a binding effect on the nanoparticles and also enhanced mobility of ionic species. Proton migration activity was influenced by the ion exchange process of ionic liquid and sulfonic acid (SO_3−) groups in addition to the hydrogen bonding network of surficial −OH groups. Despite the slight decrease in initial decomposition temperature, the membrane exhibited a relatively lower decomposition (mass loss) upon addition of the ionic liquid. This behavior is consistent with thermal properties of ionic liquid modified silica materials. Regardless of the slight decrease in proton transfer, the membrane maintained adequate conductivity up to 80 h at 160 °C under a nonexternal humidity dependent cyclic test. Anhydrous proton conductivity of the composite membrane impregnated with ionic liquid increased with the temperature from 3.57×10^{-3} S cm^{-1} at 40 °C to 1.14×10^{-2} S cm^{-1} at 160 °C. This value is comparable to the conductivity of the well studied anhydrous phosphoric acid doped polybenzimidazole membranes and is the typical value for practical fuel cell performance. Consequently, tailoring the surface properties of mesoporous SBA-16 by organic functionalization offers a convenient approach for the synthesis of SiO_2−DMPCS composite materials as proton conducting electrolytes for elevated temperature fuel cell application.

AUTHOR INFORMATION

Corresponding Author

*Tel. :+86 139 7164 3961. Fax: +86 27 87879468. E-mail: haining.zhang@whut.edu.cn.

Notes

The authors declare no competing financial interest.

ACKNOWLEDGMENTS

This work was supported by the Major State Basic Research Development Program of China "973 Project" (Grant No.: 2012CB215504) and the National Natural Science Foundation of China (No. 51372192 and No. 51376058).

REFERENCES

(1) Jochen, M.; Antje, T.; Claus, V.; Kornelia, S.; Wolfgang, L.; Dieter, L. *Sep. Purif. Technol.* **2005**, *41*, 207−220.
(2) Bijay, B. T.; Vinod, K. S. *Prog. Polym. Sci.* **2011**, *36*, 945−979.
(3) Ananta, K. M.; Saswata, B.; Tapas, K.; Nam, H. K.; Joong, H. L. *Prog. Polym. Sci.* **2012**, *37*, 842−869.
(4) Smith, B.; Sridhar, S.; Khan, A. A. *J. Membr. Sci.* **2005**, *259*, 10−26.
(5) Haile, S. M.; Boysen, D. A.; Chisholm, C. R. I.; Merle, R. B. *Nature* **2001**, *410*, 910−913.
(6) Li, Q. F.; He, R. H.; Jensen, J. O.; Bjerrum, N. J. *Chem. Mater.* **2003**, *15*, 4896−4915.
(7) Zhang, J. J.; Xie, Z.; Zhang, J. L.; Song, C.; Navessin, T.; Shi, Z.; Wang, H. J.; Wilkinson, D. P.; Liu, Z.; Holdcroft, S. *J. Power Sources* **2006**, *160*, 872−891.
(8) Ramani, V.; Kunz, H. R.; Fenton, J. M. *J. Membr. Sci.* **2004**, *232*, 31−44.
(9) Rikukawa, M.; Sanui, K. *Prog. Polym. Sci.* **2000**, *25*, 1463−1502.
(10) Mahrenia, A.; Mohamada, A. B.; Kadhum, A. A. H.; Daud, W. R. W.; Iyuke, S. E. *J. Membr. Sci.* **2009**, *327*, 32−40.

(11) Moghaddam, S.; Pengwang, E.; Jiang, Y.; Garcia, A. R.; Burnett, D. J.; Brinker, J. C.; Masel, R. I.; Shannon, M. A. *Nat. Nanotechnol.* **2010**, *5*, 230−236.
(12) Jalani, N. H.; Dunn, K.; Datta, R. *Electrochim. Acta* **2005**, *51*, 553−560.
(13) Shen, J.; Ruan, H.; Wu, L.; Gao, C. *Chem. Eng. J.* **2011**, *168*, 1272−1278.
(14) Oh, S. J.; Kim, N.; Lee, Y. T. *J. Membr. Sci.* **2009**, *345*, 13−20.
(15) Giffin, G. A.; Piga, M.; Lavina, S.; Navarra, M. A.; D'Epifanio, A.; Scrosati, B.; Noto, V. D. *J. Power Sources* **2012**, *198*, 66−75.
(16) Tang, H. L.; Pan, M. *J. Phys. Chem. C* **2008**, *112*, 11556−11568.
(17) Li, K.; Ye, G.; Pan, J.; Zhang, H.; Pan, M. *J. Membr. Sci.* **2010**, *347*, 26−31.
(18) Li, Q.; Xiao, C.; Zhang, H.; Chen, F.; Fang, P.; Pan, M. *J. Power Sources* **2011**, *196*, 8250−8256.
(19) Wang, L.; Zhao, D.; Zhang, H. M.; Xing, D. M.; Yi, B. L. *Electrochem. Solid-State Lett.* **2008**, *11*, B201−B204.
(20) Steele, B. C.; Heinzel, A. *Nature* **2001**, *414*, 345−352.
(21) Zhuravlev, L. T. *Colloids Surf., A* **2000**, *173*, 1−38.
(22) Dugas, V.; Chevalier, Y. *J. Colloid Interface Sci.* **2003**, *264*, 354−361.
(23) El-Nahhal, I. M.; El-Ashgar, N. M. *J. Organomet. Chem.* **2007**, *692*, 2861−2886.
(24) Ruiz-Hitzky, E. Organic-Inorganic Materials: From Intercalation Chemistry to Devices. In *Functional Hybrid Materials*; Gómez-Romero, P., Sanchez, C., Eds.; Wiley-VCH Verlag GmbH & Co. KGaA: Weinheim, Germany, 2004; pp 27−32.
(25) Wu, Q. X.; Zhao, T. S.; Chen, R.; Yang, W. W. *Int. J. Hydrogen Energy* **2010**, *35*, 10547−10555.
(26) Jung, D. H.; Cho, S. Y.; Shin, D. R.; Kim, J. S. *J. Power Sources* **2002**, *106*, 173−177.
(27) Tang, H.; Pan, M.; Lu, S.; Lu, J.; Jiang, S. *Chem. Commun.* **2010**, *46*, 4351−4353.
(28) Halla, J. D.; Mamak, M.; Williams, D. E.; Ozin, G. A. *Adv. Funct. Mater.* **2003**, *13*, 133−138.
(29) Marschall, R.; Tolle, P.; Cavalcanti, W. L.; Wilhelm, M.; Kohler, C.; Frauenheim, T.; Wark, M. *J. Phys. Chem. C* **2009**, *113*, 19218−19227.
(30) Sharifi, M.; Kohler, C.; Tolle, P.; Frauenheim, T.; Wark, M. *Small* **2011**, *7*, 1086−1097.
(31) Sel, O.; Azais, T.; Marechal, M.; Gebel, G.; Laberty-Robert, C.; Sanchez, C. *Chem. Asian J.* **2011**, *6*, 1992−3000.
(32) Pan, Y. C.; Tsai, H. H. G.; Jiang, J. C.; Kao, C. C.; Sung, T. L.; Chiu, P. J.; Saikia, D.; Chang, J. H.; Kao, H. M. *J. Phys. Chem. C* **2012**, *116*, 1658−1669.
(33) Marschall, R.; Sharifi, M.; Wark, M. *Microporous Mesoporous Mater.* **2009**, *123*, 21−29.
(34) Mishra, A. K.; Kuila, T.; Kim, D. Y.; Kim, N. H.; Lee, J. H. *J. Mater. Chem.* **2012**, *22*, 24366−24372.
(35) Lu, F.; Gao, X.; Yan, X.; Gao, H.; Shi, L.; Jia, H.; Zheng, L. *ACS Appl. Mater. Interfaces* **2013**, *5*, 7626−7632.
(36) Li, H.; Tang, Y.; Wang, Z.; Shi, Z.; Wu, S.; Song, D.; Zhang, J.; Fatih, K.; Zhang, J.; Wang, H.; Liu, Z.; Abouatallah, R.; Mazza, A. *J. Power Sources* **2008**, *178*, 103−117.
(37) Stevens, W. J. J.; Mertens, M.; Mullens, S.; Thijs, I.; Tendeloo, G. V.; Cool, P.; Vansant, E. F. *Microporous Mesoporous Mater.* **2006**, *93*, 119−124.
(38) Tachikawa, M. Method of making an aromatic chlorosilane compound by a hydrosilation reaction. U. S. Patent 6,054,602, April 25, 2000.
(39) Sun, H.; Tang, Q.; Du, Y.; Liu, X.; Chen, Y.; Yang, Y. *J. Colloid Interface Sci.* **2009**, *333*, 317−323.
(40) Aburto, J.; Ayala, M.; Bustos-Jaimes, I.; Montiel, C.; Terres, E.; Dominguez, J. M. *Microporous Mesoporous Mater.* **2005**, *83*, 193−200.
(41) Wang, L.; Fan, J.; Tian, B.; Yang, H.; Yu, C.; Bo, T.; Zhao, D. *Microporous Mesoporous Mater.* **2004**, *67*, 135−141.
(42) Hoffmann, F.; Cprnelius, M.; Morell, J.; Froba, M. *Angew. Chem., Int. Ed.* **2006**, *45*, 3216−3251.
(43) Brindle, R.; Pursch, M.; Albert, K. *Solid State Nucl. Magn. Reson.* **1996**, *6*, 251−266.
(44) Siegel, R.; Domingues, E.; Sousa, R. D.; Jerome, F.; Morais, C. M.; Bion, N.; Ferreira, P.; Mafra, L. *J. Mater. Chem.* **2012**, *22*, 7412−7419.
(45) Pardal, F.; Lapinte, V.; Robin, J. J. *J. Polym. Sci., Part A: Polym. Chem.* **2009**, *47*, 4617−4628.
(46) Kreuer, K. D.; Schuster, M.; Obliers, B.; Diat, O.; Traub, U.; Fuchs, A.; Klock, U.; Paddison, S. J.; Maier, J. *J. Power Sources* **2008**, *178*, 499−509.
(47) Fujita, S.; Koiwai, A.; Kawasumi, M.; Inagaki, S. *Chem. Mater.* **2013**, *25*, 1584−1591.
(48) Li, Q.; Jensen, J. O.; Savinell, R. F.; Bjerrum, N. J. *Prog. Polym. Sci.* **2009**, *34*, 449−477.
(49) Li, W.; Zhang, F.; Yi, S.; Huang, C.; Zhang, H.; Pan, M. *Int. J. Hydrogen Energy* **2011**, *37*, 748−754.
(50) Fujita, S.; Kamazawa, K.; Yamamoto, S.; Tyagi, M.; Araki, T.; Sugiyama, J.; Hasegawa, N.; Kawasumi, M. *J. Phys. Chem. C* **2013**, *117*, 8727−8736.
(51) Shvedene, N. V.; Chernyshev, D. V.; Gromova, Yu P.; Nemilova, Mu Y.; Pletnev, I. V. *J. Anal. Chem.* **2010**, *65*, 861−865.
(52) Ye, Y. S.; Rick, J.; Hwang, B. J. *J. Mater. Chem. A* **2013**, *1*, 2719−2734.